Peer-reviewed version available at *Biosensors* **2018**, *9*, 4; doi:10.3390/bios9010004

Article

ZIF Nanocrystal-Based SAW Electronic Nose to Detect Diabetes in Human Breath

Fabio A. Bahos[1], Arianee Sainz-Vidal[1], Celia Sánchez-Pérez[1], José M. Saniger[1], Isabel Gràcia[2], María M. Saniger-Alba[3], Daniel Matatagui[1,4]*

[1] Instituto de Ciencias Aplicadas y Tecnología (ICAT), Universidad Nacional Autónoma de México, CU 04510, Cd. México, México
[2] Instituto de Microelectrónica de Barcelona (IMB), CSIC, Campus UAB, 08193, Bellaterra, Spain
[3] Instituto Nacional de la Nutrición Salvador Zubiran, Department of Neurophysiology, Tlalpan 14080, México
[4] SENSAVAN, Instituto de Tecnologías Físicas y de la Información (ITEFI), CSIC, Serrano 144, 28006, Madrid, Spain
* Correspondence: d.m@csic.es; Tel.: (+34) 91 561 88 06 Ext.: 920422

Abstract:

In the present work a novel, portable and innovative eNose composed of a surface acoustic wave (SAW) sensor array based ZIF-8, and ZIF-67 nanocrystals (pure and combined with gold nanoparticles) as sensitive layers has been tested as a non-invasive system to detect and differentiate disease markers, such as acetone, ethanol and ammonia, related with diagnosis and control of diabetes mellitus through exhaled breath. The sensors have been prepared by spin coating, achieving continuous and homogenous sensitive layers. Low concentrations (5 ppm, 10 ppm and 25ppm) of the marker analytes were measured, obtaining high sensitivities, good reproducibility, short time response and fast signal recovery.

Keywords: eNose; gas sensor, SAW; Surface Acoustic Wave, Love wave, diabetes, breath, VOC, ZIF, Zeolite

1. Introduction

Nowadays one of the great challenges of science is the diagnosis of diseases in the least amount of time and using non-invasive techniques. This strategy intends to provide a higher quality of life for humans and reduce the mortality rate. Additionally, an early treatment of diseases and its complications has an important economic impact by helping to avoid or reduce treatment costs.
The last portion of deeply exhaled breath, representing alveolar air, can be considered the headspace gas of blood. Exhaled breath, recognized mainly through the sense of smell, is a method used for a long time to disease diagnosis. This method was abandoned due to the emergence of new accurate and effective techniques, despite the fact that any of them were highly invasive. Over the last few decades, an important advance in the gas analysis technologies has re-launched the idea to diagnose diseases through exhaled breath. Various studies conducted by these analysis techniques, such as gas chromatography-mass spectrometry (GC-MS), proton transfer reaction-mass spectrometry (PTR-MS), selected ion flow tube-mass spectrometry (SIFT-MS), ion mobility and optical absorption[1–5], have shown a link between the chemical composition of the exhaled breath and certain diseases, chemical compounds present in the exhaled breath that change due to diseases are known as markers. The above conventional systems are accurate, but they are also bulky, expensive, and require highly-qualified operators, facts that increase the demand of low-cost systems with high sensitivity and low dimensionality based on solid-state chemical sensors, with different detection principles such as impedance [6], resistive [7,8], optical [9] and piezoelectric [10,11], surface acoustic wave (SAW) being one of the most sensitive devices among piezoelectric ones [12]. At the nanoscale, materials and their advanced design features have led to a new generation of chemical sensors with enhanced sensitivity

and response time [13–15]. Due to its unique porous structure zeolites have been used to detect gases [16]. However, in the last years, organic zeolites such as zeolitic imidazolate frameworks (ZIFs) have attracted major attention as gas detectors [17], because they offer two primary advantages over conventional zeolites. First, they have larger porous size (about 1.16 nm for ZIF-8 and ZIF-67) and usually smaller crystal size, resulting in higher surface area. Second, hydrophobic behaviour is more pronounced in many ZIFs [18,19].

The World Health Organization (WHO) recognize diabetes mellitus, known as diabetes, as a serious and chronic disease that in 2012 caused 1.5 million deaths. A recent study from reports in 2015 of 111 countries, estimated that there were 415 million people with diabetes aged 20–79 years, 5 million of deaths attributable to diabetes, and the total global health expenditure due to diabetes was estimated on 673 billion US dollars representing a substantial clinical and public health burden [8]. Moreover, the number of cases of diabetes among youths [20] and infancy [21] increased in recent years but recent incidence trends are lacking and only statistical data for some countries are available.

The presence of ketones in the exhaled breath is a warning sign of ketosis that is related to fat catabolism either due to carbohydrate deprivation or to its lack of utilization in persons with diabetes. This condition is known as diabetic ketoacidosis and requires immediate treatment. One type of ketone, known as acetone, provides a non-invasive measure of ketosis through breath. The basal level of acetone in a healthy situation can be around 2 ppm [5,22]. Adults following low-carbohydrate diets can have elevated levels of up to 40 ppm [23–25], and poorly controlled diabetes can cause ketoacidosis which can increase acetone concentration up to 1250 ppm [22,26]. However, human exhaled air is a complex mixture of chemical compounds, making the detection and stage classification of a determinate disease through a unique marker difficult, and, consequently different disease markers need to be considered as indicators. Another marker related with blood glucose concentration and present in exhaled breath is ethanol. Though ethanol is not directly produced by any known mammalian cellular biochemical pathway, it may increase in exhaled gas mixtures because of alcoholic fermentation of an excessive overload of carbohydrate-rich food in conjunction with overgrowth of intestinal bacteria. Ethanol used in combination with exhaled acetone allowed the prediction of fluctuating plasma glucose concentrations in a multi-linear regression model [27–30], therefore it could be helpful for determining diabetes through breath. On the other hand, diabetes represents the cause of half of cases of renal failure cases. Kidney failure is related with ammonia levels higher than 3 ppm in exhaled breath [5,25,31,32]. Consequently, a finger print using breath levels of acetone, ethanol and ammonia could be a non-invasive predictor of diabetes, its control, and a proxy of damage of the disease.

In the present work, a SAW eNose, based on ZIF nanocrystals as sensitive layers, has been tested to acetone, ethanol, and ammonia as a potential non-invasive system to the diabetes diagnosis and conrol.

2. Materials and Methods

2.1. Materials

All the reagents were purchased from a commercial provider (Sigma-Aldrich) and used without further purification, including $ZnCl_2$ (98%), $CoCl_2{\cdot}6H_2O$ (98%), and 2methylimidazole (99%), hydrogen tetrachloroaurate (III) hydrate ($HAuCl_4$, 99.9%) and trisodium citrate dihydrate ($HOC(COONa)(CH_2COONa)_2 \cdot 2H_2O$).

2.2. Synthesis of ZIF-8 and ZIF-67

ZIF-8 and ZIF-67 samples were synthesized using the aqueous method reported elsewhere [33]. For ZIF-8 synthesis, a solution of 1.17 g of zinc chloride dissolved in 8 mL DI water was added into a solution of 2-methylimidazole (2MeIM) (22.70 g) dissolved in 80 mL DI water, to yield a molar ratio of 2-methylimidazole to zinc of 70:1. The mixture was stirred at room temperature for 5 min. The product was collected by centrifugation (24000 rpm, 10min), washed in DI water three times and dried at 65°C for 24h in an oven. ZIF-67 was synthesized identically to the ZIF-8 material as described

above, now replacing zinc chloride with the equivalent quantity of cobalt chloride hexahydrate. A scheme of the synthesis paths is described in Fig. 1 [34,35].

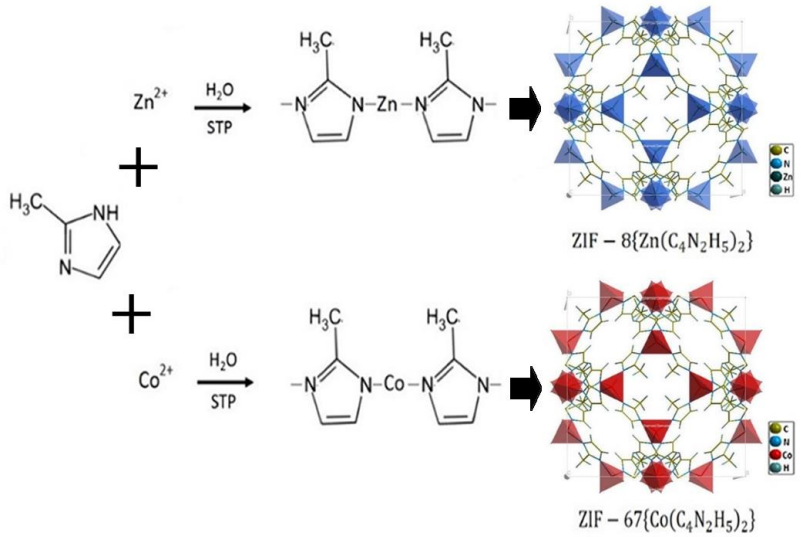

Figure 1. Representative synthesis and crystal structures of ZIF-8 and ZIF-67 used as the sensitive layers of gas sensors.

2.3. Synthesis of gold nanoparticles

Gold nanoparticles (AuNP) were prepared according to the procedure described in reference [36]. An aqueous solution of $HAuCl_4$ (0.001M, 40 mL) was placed into a 250 mL round bottom flask. The solution was heated to 90 °C followed by the addition of sodium citrate aqueous solution (38.8mM, 2 mL) into it while stirring for 15min. After cooling down to room temperature, the solution was centrifuged three times with ethanol and three times with DI water, finally the precipitate was redispersed in DI water, resulting a water solution with AuNP of ~5 nm.

2.4. ZIFs nanocrystal characterization

The synthetized samples were kept at room conditions and characterized using: Fourier transform-infrared spectroscopy (FTIR), X-ray diffraction (XRD), scanning electron microscope (SEM) and energy-dispersive X-ray (EDS). FTIR spectra were recorded using a Thermo Nicolet NEXUS 670 FTIR spectrometer. The sample was diluted into KBr pellets in a 1:100 weight ratio (sample to KBr). The scanning range was 400–4000 cm^{-1} and the resolution was 4 cm^{-1}. XRD powder patterns were recorded with CuKα radiation in a D8 advance diffractometer from Bruker. The morphological features were examined by SEM. The SEM and EDS analysis were performed on a JEOL JMS-7600F.

2.5. Love-wave sensor

Love-wave (LW) are a specific type of SAW sensors based on shear horizontal (SH) waves guided by a layer with a lower propagation velocity than the piezoelectric substrate. The energy of the wave is confined in the guiding layer and any perturbation in it affects the acoustic wave velocity. The LW sensors used in the present work were designed with a delay line (DL) configuration. This device is based on a micro-electromechanical system composed of a piezoelectric material (ST-Quartz) with facing input/output aluminium interdigital transducers (IDT) on its surface, working at a 28 μm wavelength (λ), with a separation between its IDTs of 2100 μm (Fig. 2a). The SH waves were guided by a 3.1 μm thick layer of SiO_2, on which sensitive layers were deposited. An oscillator circuit consisting of a DL, with an amplification stage and a coupler were used for measuring the changes in the velocity of the waves by means of the resonant frequency (Fig. 2b).

Peer-reviewed version available at Biosensors 2018, 9, 4; doi:10.3390/bios9010004

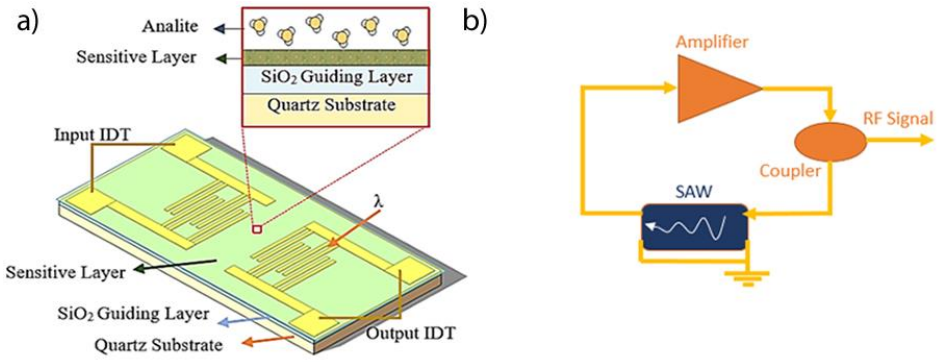

Figure 2. a) Scheme representation of LW sensor and layer composition. b) Oscillator circuit used to read the resonant frequency.

2.6. ZIF as sensitive layers

The eNose was based on a SAW sensor array with different sensitive layers to achieve a specific fingerprint for analytes of interest. The sensitive material samples were obtained mixing each main solution with a volumetric proportion of 75% (solution-1) and 25% (solution-2) (Table 1). Spin coating technique was used to deposit a thin layer of sensitive material. The process consisted of putting sample drops directly on the SiO_2 guiding layer, and then the assemblage is rotated at a speed of 3000 rpm during one minute (Fig. 3). A suitable thickness for each sensor is obtained after depositing four times in a multilayer configuration achieving an optimal sensitivity for sensors. After ZIFs deposition process a thermal treatment at 180 °C with 50 ml/min nitrogen flow in a tubular oven was applied during 4 hours for extracting the excess of the 2MeIM organic ligand in the sensitive layer.

Table 1. Different composition of the sensitive layers used in the SAW sensors included in the eNose..

Samples	Solución-1 (750 µl)	Solución-2 (250 µl)
S_1	ZIF-67	Au-NPs
S_2	ZIF-8	Au-NPs
S_3	ZIF-67	H_2O-DI
S_4	ZIF-8	H_2O-DI

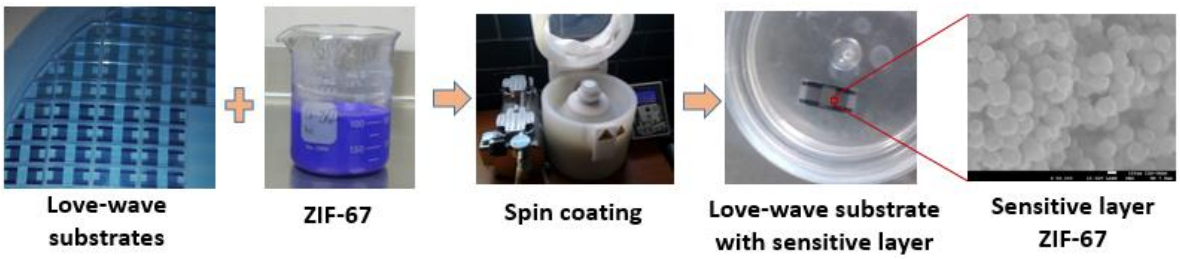

Figure 3. Process sequence of sensitive layer deposition on LW devices by means spin coating technique.

2.7. Experimental setup

The sensor array was tested to acetone, ethanol, and ammonia gas analytes diluted in synthetic dry air to obtain the required concentrations: 5 ppm, 10 ppm, and 25 ppm. The gas sample generator (Fig. 4) consists of two mass flow controllers, which were utilized for obtaining desirable concentrations at a constant flow of 100 ml/min. For the detection, a sensing system composed of a measuring instrument (eNose) manufactured to be operated with a SAW sensor array was used. Finally, sensor responses were acquired by a micro-frequency counter, and the information was

transmitted wirelessly. A custom application was developed to display and store the sensor data in real time.

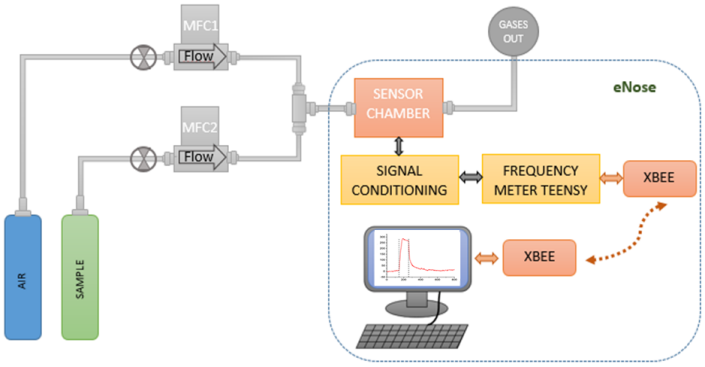

Figure 4. Diagram of instrumentation and experimental setup for the eNose characterization.

3. Results and Discussion

3.1. Structural and morphological characterization of ZIFs

The FTIR spectra of KBr diluted ZIF-8 and ZIF-67 samples show the characteristics adsorption bands of 2meImidazole ring vibrations, reported for this structures in previous works [37] (Fig. 5a). The XRD patterns of both ZIFs samples evidence the formation of a largely crystalline structure with long-range order (Fig. 5b) The position and relative intensity of the diffraction maxima are in correspondence with the literature statements for ZIF-8 and ZIF-67 frameworks [34,37,38].

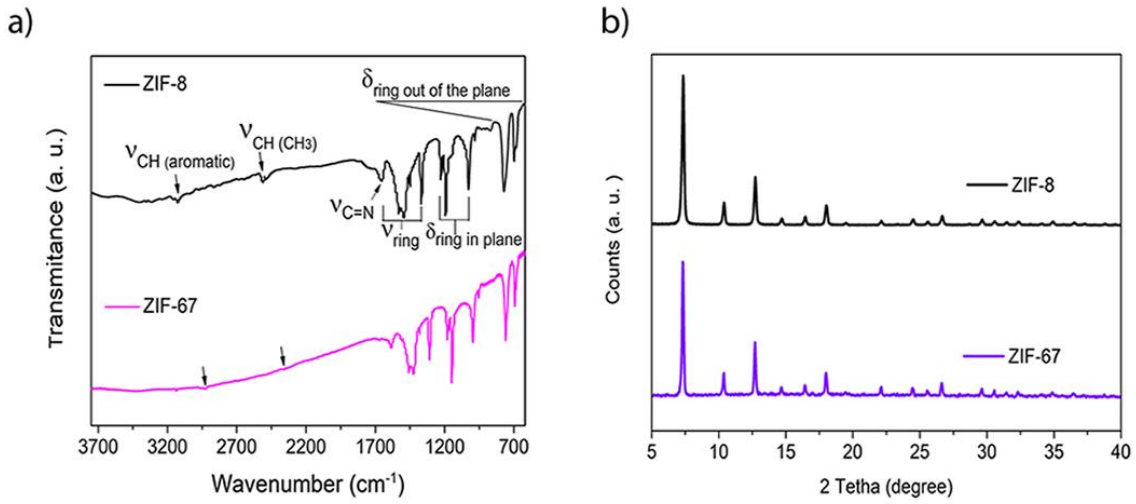

Figure 5. (a) FTIR spectra of the ZIF-8 and ZIF-67 samples diluted in KBr. (b) 2- XRD Powder Pattern of the ZIF-8 and ZIF-67 samples.

SEM images exhibited that the nanocrystals were configured like a continuous layer with very small particles (Fig. 6a). This fact is important because nanostructured layers had two advantages: first, the surface area of reaction with the gaseous environment is higher; second, the wave is propagated as in a continuous layer with very low scattering due to its wavelength (28 μm), which is much higher than the diameter of the nanocrystals. The micrographs also showed hexagonal shaped nanocrystals of 50 nm approx. for the ZIF-8 samples (Fig. 6b) and 200 nm approx. for the ZIF-67 samples (Fig. 6c).

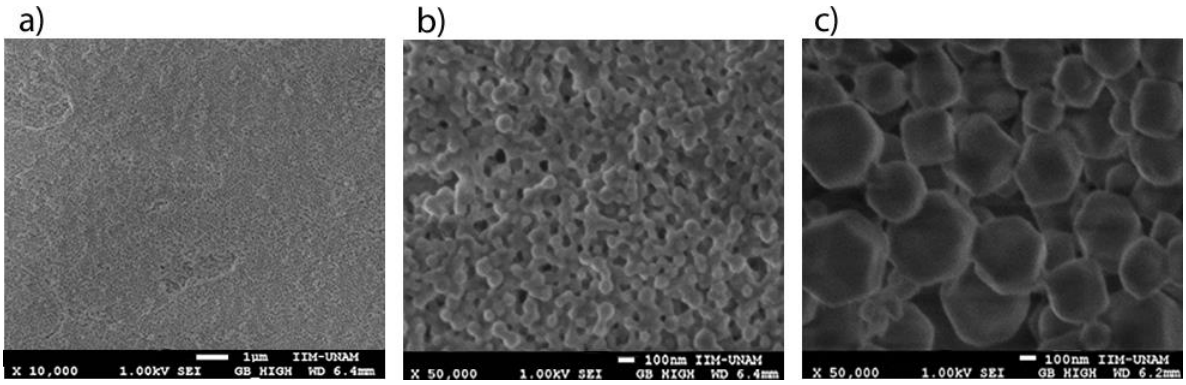

Figure 6. SEM image with magnification of (a) 10,000× for a continuous layer of ZIF-8 nanocrystals, (b) 50,000× for a layer of ZIF-8 nanocrystals and (c) 50,000× for a layer of ZIF-67 nanocrystals.

3.2. *Electrical characterization of the Love wave sensors*

The LW sensors were characterized before and after depositing the ZIF nanocrystals sensitive layers. In the array, a reference device without sensitive layer was used (Fig. 7a) to compensate sensor responses for undesirable changes in temperature and pressure. The sensors were characterized by means of the automatic network analyzer (ANA Wiltron 360B) and the S21 parameter was used to measure insertion loss transmission. The frequency response of each sensor exhibited a frequency shift of the minimum insertion loss occasioned by the mass loading of the sensitive material (Fig. 7b and c). On the other hand, increases of insertion losses (Table 2) were a consequence of the scattering due to the propagation of the SAW wave in the sensitive material.

Table 2. Insertion loss and frequency shift with respect to the reference sensor, 165 MHz and 18.3 dB.

Sensors	Sensitive layer	Insertion loss (dB)	Frequency shift (Hz)
S1	ZIF-67+AuNPs	3.4	1100
S2	ZIF-8+AuNPs	2.6	2400
S3	ZIF-67+H2O	7.1	900
S4	ZIF-8+H2O	8.7	1500

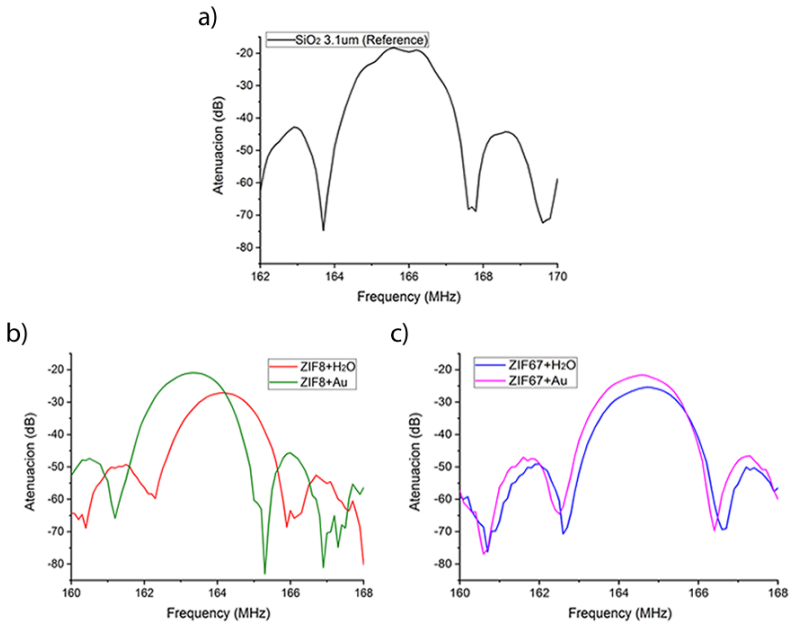

Figure 7. Spectral response of the LW sensors (a) without (b) and (c) with sensitive layers.

3.3. Gas characterization

The SAW eNose based on a LW sensor array with ZIFs nanocrystals was tested to acetone, ethanol and ammonia markers related to diabetes mellitus disease. The sensors were exposed during two minutes to each analyte at concentrations of 5 ppm, 10 ppm and 25 ppm, and then the array was purged with dry synthetic air for 10 minutes. The LW sensors showed a notable and fast response, e.g., for 10 ppms of acetone a frequency shift of 275 Hz and a τ_{90}, around 30 s, with a complete recovery achieved after 10 min (Fig. 8a), τ_{90} being defined as the time taken to reach the 90% of the frequency shift. The response of the sensor array to different concentrations of acetone (Fig. 8b), ethanol (Fig. 8c), and ammonia (Fig. 8d) showed a high frequency shift for the different sensitive layers tested, obtaining best sensitivities for S_2 (ZIF67_Au) and higher responses for higher concentrations. Therefore, the eNose could be used to make a diagnosis in a few seconds and be repeated or carry out a new diagnosis after ten minutes.

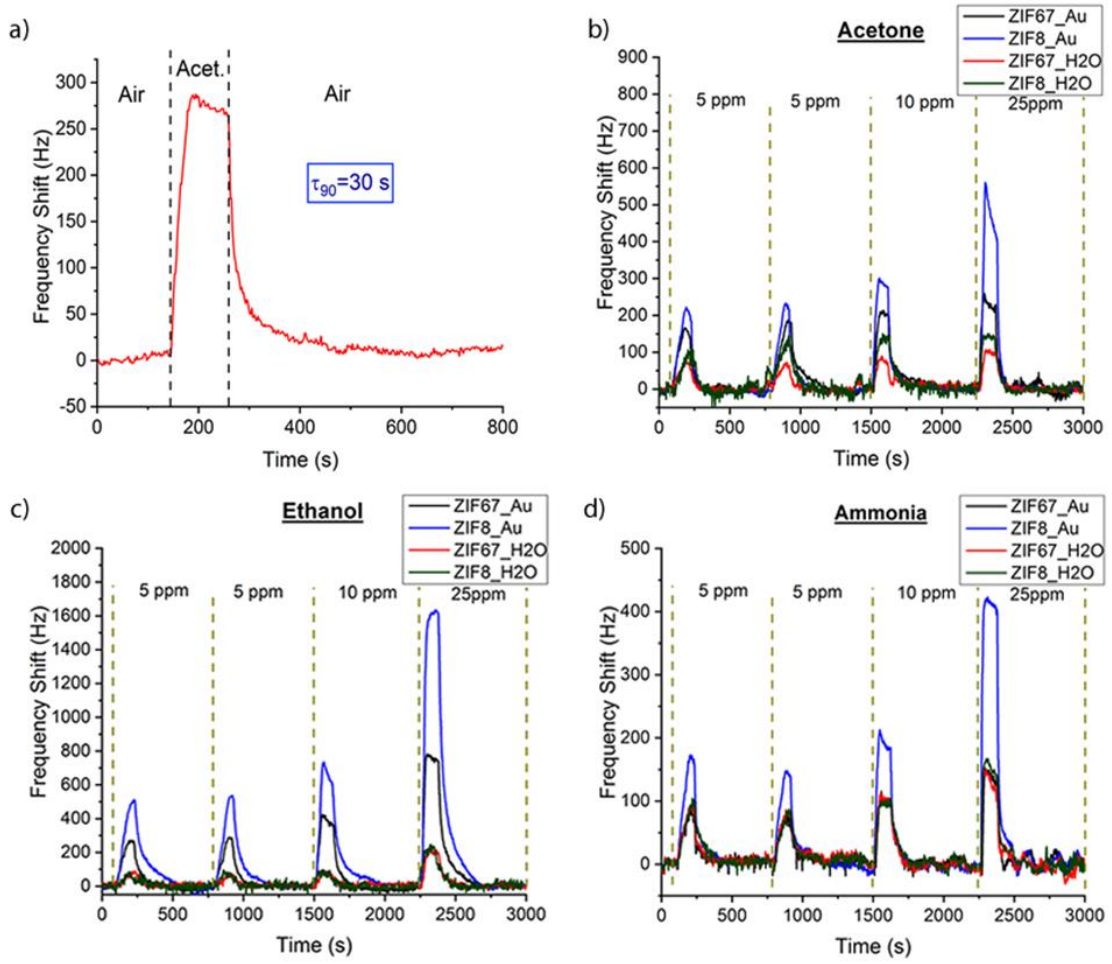

Figure 8. (a) SAW eNose response to 10 ppm of acetone. Experimental response for 5 ppm, 10 ppm and 25 ppm of (b) acetone, (c) ethanol and (d) ammonia with S1, S2, S3, and S4 sensitive layers.

The reference sensor helped to compensate in the sensor array the pressure and temperature changes due to external factors, measuring only variations related to the interaction of the analytes with the sensitive layers. The noise level for LW sensors is 10 Hz/min, thus the minimum detectable measurement, three times signal-to-noise ratio, is a frequency shift of 30 Hz, obtaining the lowest detection limits for the sensor based on ZIF-8/AuNP, at 0.7 ppm, 0.3 ppm and 1 ppm for acetone, ethanol and ammonia, respectively. Therefore, sensors with nanocrystalline ZIF as sensitive materials allowed for the detection and discrimination of acetone, ammonia, and ethanol, as shown in the radial surface analysis to 10 ppm of the three markers (Fig. 9), therefore, the SAW eNose presented could be used to relate determined fingerprints with diabetes diseases.

Peer-reviewed version available at Biosensors 2018, 9, 4; doi:10.3390/bios9010004

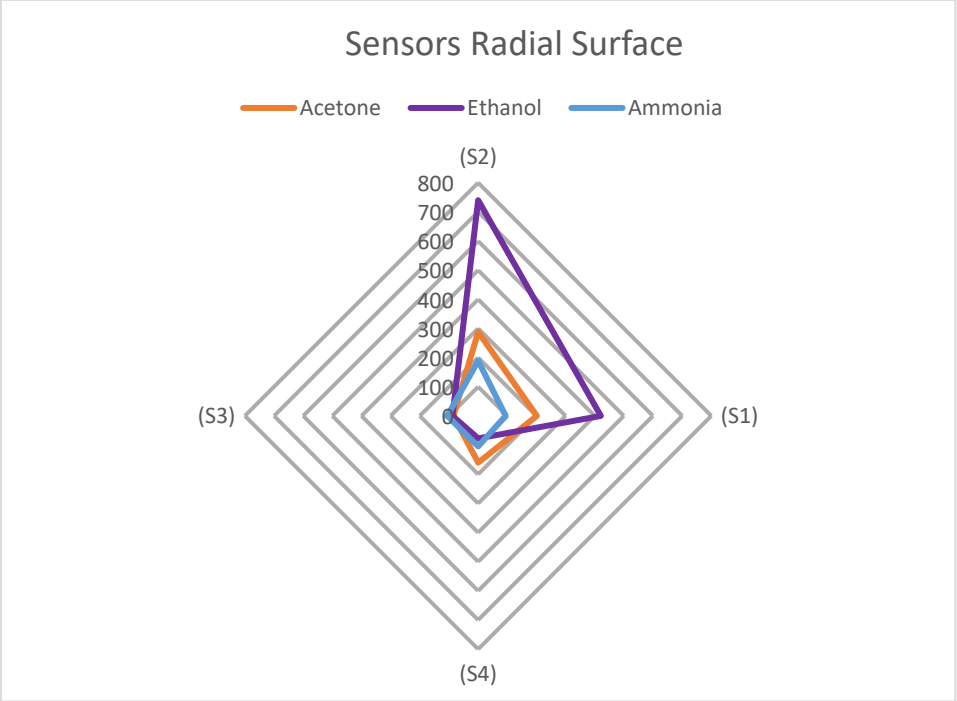

Figure 9. Radial representation of the sensor array responses to 10 ppm of acetone, ethanol and ammonia.

4. Conclusions

A SAW eNose based on Love wave sensors combined with ZIF-8, ZIF-67, ZIF-8/AuNP and ZIF-67/AuNP as sensitive layers was tested to three breath markers of diabetes mellitus: acetone, ethanol and ammonia at concentrations of 5 ppm, 10 ppm and 25 ppm. These diabetes markers were detected with fast response time, around 30 s, and a complete recovery time, below 10 min. In addition, sensor array response showed as each marker has its own fingerprint. In conclusion, tests carried out in this work shows a properly performance of the SAW/ZIF eNose to be proved in future works as a prototype for a noninvasive system contributing to the diagnosis and control of diabetes mellitus in real cases.

Author Contributions: Fabio Bahos and Daniel Matatagui designed and developed the instrumentation, and they measured the disease markers. Arianee Sainz and José Saniger designed and synthesized the nanomaterials. Celia Sánchez, José Saniger and Daniel Matatagui designed and directed the research. Isabel Gràcia fabricated the SAW devices. María del Mar Saniger Alba provided a medical overview focus on the application of the eNose for the diabetes diagnosis and control. All authors have participated in the discussions of the results and have approved the final version of the manuscript.

Funding: This work has been supported by Universidad Nacional Autónoma de México via Grants DGAPA-UNAM-PAPIIT TA100118 and DGAPA-UNAM-PAPIIT IT100518, the Fundación General CSIC via Programa ComFuturo, and the Spanish Ministry of Science and Innovation via Grant TEC2016-79898-C6-(AEI/FEDER,EU). This research has used the Spanish ICTS Network MICRONANOFABS (partially funded by MINECO).

Acknowledgments: FABH thanks to CONACYT-México for his master. AS thanks to CONACYT- México by her posdoctoral grant. A. Sainz-Vidal acknowledge CONACYT project 2014-Fronteras 2016-01 for the postdoctoral fellowship. FABH, ASV, JMS and DM thank to the Laboratorio Universitario de Caracterización Espectrocópica (LUCE) by the use of its facilities and Selene Islas, V. Maturano, M. E. Mata Zamora and J.O. Flores-Flores for their technical assistance, as well as to Antonio Morales for the DRX measurements at the IF-UNAM and to Omar Novelo for the SEM and EDS measurements at the IIM-UNAM.

Conflicts of Interest: There are no conflicts of interest.

References

1. Dummer, J.; Storer, M.; Swanney, M.; McEwan, M.; Scott-Thomas, A.; Bhandari, S.; Chambers, S.; Dweik, R.; Epton, M. Analysis of biogenic volatile organic compounds in human health and disease. *TrAC Trends Anal. Chem.* **2011**, *30*, 960–967, doi:10.1016/J.TRAC.2011.03.011.

2. Cikach, F. S.; Dweik, R. A. Cardiovascular Biomarkers in Exhaled Breath. *Prog. Cardiovasc. Dis.* **2012**, *55*, 34–43, doi:10.1016/J.PCAD.2012.05.005.

3. Miekisch, W.; Schubert, J. K. From highly sophisticated analytical techniques to life-saving diagnostics: Technical developments in breath analysis. *TrAC Trends Anal. Chem.* **2006**, *25*, 665–673, doi:10.1016/J.TRAC.2006.05.006.

4. Das, S.; Pal, S.; Mitra, M. Significance of Exhaled Breath Test in Clinical Diagnosis: A Special Focus on the Detection of Diabetes Mellitus. *J. Med. Biol. Eng. 36*, doi:10.1007/s40846-016-0164-6.

5. Diskin, A. M.; pan l, P.; Smith, D. Time variation of ammonia, acetone, isoprene and ethanol in breath: a quantitative SIFT-MS study over 30 days. *Physiol. Meas.* **2003**, *24*, 107–119, doi:10.1088/0967-3334/24/1/308.

6. Rheaume, J. M.; Pisano, A. P. A review of recent progress in sensing of gas concentration by impedance change. *Ionics (Kiel).* **2011**, *17*, 99–108, doi:10.1007/s11581-010-0515-1.

7. Santos, J. P.; Fernández, M. J.; Fontecha, J. L.; Matatagui, D.; Matatagui, D.; Sayago, I.; Horrillo, M. C.; Gracia, I. Nanocrystalline tin oxide nanofibers deposited by a novel focused electrospinning method. Application to the detection of TATP precursors. *Sensors (Switzerland)* **2014**, *14*, doi:10.3390/s141224231.

8. Nayak, A. K.; Ghosh, R.; Santra, S.; Guha, P. K.; Pradhan, D. Hierarchical nanostructured WO_3–SnO_2 for selective sensing of volatile organic compounds. *Nanoscale* **2015**, *7*, 12460–12473, doi:10.1039/C5NR02571K.

9. Hodgkinson, J.; Tatam, R. P. Optical gas sensing: a review. *Meas. Sci. Technol.* **2013**, *24*, 012004, doi:10.1088/0957-0233/24/1/012004.

10. Hromadka, J.; Tokay, B.; Correia, R.; Morgan, S. P.; Korposh, S. Highly sensitive volatile organic compounds vapour measurements using a long period grating optical fibre sensor coated with metal organic framework ZIF-8. *Sensors Actuators B Chem.* **2018**, *260*, 685–692, doi:10.1016/J.SNB.2018.01.015.

11. Fragoso-Mora, J. R.; Matatagui, D.; Bahos, F. A.; Fontecha, J.; Fernandez, M. J.; Santos, J. P.; Sayago, I.; Gràcia, I.; Horrillo, M. C. Gas sensors based on elasticity changes of nanoparticle layers. *Sensors Actuators, B Chem.* **2018**, *268*, doi:10.1016/j.snb.2018.04.045.

12. Ballantine, D. S.; Martin, S. J.; Ricco, A. J.; Frye, G. C.; Wohltjen, H.; White, R. M.; Zellers, E. T. Chapter 3 - Acoustic Wave Sensors and Responses. In *Applications of Modern Acoustics*; Ballantine, D. S., Martin, S. J., Ricco, A. J., Frye, G. C., Wohltjen, H., White, R. M., Zellers, E. T. B. T.-A. W. S., Eds.; Academic Press: Burlington, 1997; pp. 36–149 ISBN 978-0-12-077460-9.

13. Kannan, P. K.; Late, D. J.; Morgan, H.; Rout, C. S. Recent developments in 2D layered inorganic nanomaterials for sensing. *Nanoscale* **2015**, *7*, 13293–13312, doi:10.1039/C5NR03633J.

14. Jiménez-Cadena, G.; Riu, J.; Rius, F. X. Gas sensors based on nanostructured materials. *Analyst* **2007**, *132*, 1083, doi:10.1039/b704562j.

15. Comini, E. Metal oxide nanowire chemical sensors: innovation and quality of life. *Mater. Today* **2016**, *19*, 559–567, doi:10.1016/J.MATTOD.2016.05.016.

16. Xu, X.; Wang, J.; Long, Y.; Xu, X.; Wang, J.; Long, Y. Zeolite-based Materials for Gas Sensors. *Sensors* **2006**, *6*, 1751–1764, doi:10.3390/s6121751.

17. Kreno, L. E.; Leong, K.; Farha, O. K.; Allendorf, M.; Van Duyne, R. P.; Hupp, J. T. Metal–Organic Framework Materials as Chemical Sensors. *Chem. Rev.* **2012**, *112*, 1105–1125, doi:10.1021/cr200324t.

18. Zhang, K.; Lively, R. P.; Zhang, C.; Chance, R. R.; Koros, W. J.; Sholl, D. S.; Nair, S. Exploring the Framework Hydrophobicity and Flexibility of ZIF-8: From Biofuel Recovery to Hydrocarbon Separations. *J. Phys. Chem. Lett.* **2013**, *4*, 3618–3622, doi:10.1021/jz402019d.

19. Eum, K.; Jayachandrababu, K. C.; Rashidi, F.; Zhang, K.; Leisen, J.; Graham, S.; Lively, R. P.; Chance, R. R.; Sholl, D. S.; Jones, C. W.; Nair, S. Highly Tunable Molecular Sieving and Adsorption Properties of Mixed-Linker Zeolitic Imidazolate Frameworks. *J. Am. Chem. Soc.* **2015**, *137*, 4191–4197, doi:10.1021/jacs.5b00803.

20. Mayer-Davis, E. J.; Lawrence, J. M.; Dabelea, D.; Divers, J.; Isom, S.; Dolan, L.; Imperatore, G.; Linder, B.; Marcovina, S.; Pettitt, D. J.; Pihoker, C.; Saydah, S.; Wagenknecht, L. Incidence Trends of Type 1 and Type 2 Diabetes among Youths, 2002–2012. *N. Engl. J. Med.* **2017**, *376*, 1419–1429, doi:10.1056/NEJMoa1610187.

21. Letourneau, L. R.; Carmody, D.; Wroblewski, K.; Denson, A. M.; Sanyoura, M.; Naylor, R. N.; Philipson, L. H.; Greeley, S. A. W. Diabetes Presentation in Infancy: High Risk of Diabetic Ketoacidosis. *Diabetes Care* **2017**, *40*, e147–e148, doi:10.2337/dc17-1145.

22. Anderson, J. C.; Lamm, W. J. E.; Hlastala, M. P. Measuring airway exchange of endogenous acetone using a single-exhalation breathing maneuver. *J. Appl. Physiol.* **2006**, *100*, 880–889, doi:10.1152/japplphysiol.00868.2005.

23. Freund, G.; Weinsier, R. L. Standardized ketosis in man following medium chain triglyceride ingestion. *Metabolism* **1966**, *15*, 980–991, doi:10.1016/0026-0495(66)90046-1.

24. Saslow, L. R.; Kim, S.; Daubenmier, J. J.; Moskowitz, J. T.; Phinney, S. D.; Goldman, V.; Murphy, E. J.; Cox, R. M.; Moran, P.; Hecht, F. M. A Randomized Pilot Trial of a Moderate Carbohydrate Diet Compared to a Very Low Carbohydrate Diet in Overweight or Obese Individuals with Type 2 Diabetes Mellitus or Prediabetes. *PLoS One* **2014**, *9*, e91027, doi:10.1371/journal.pone.0091027.

25. Phinney, S. D.; Bistrian, B. R.; Wolfe, R. R.; Blackburn, G. L. The human metabolic response to chronic ketosis without caloric restriction: Physical and biochemical adaptation. *Metabolism* **1983**, *32*, 757–768,

doi:10.1016/0026-0495(83)90105-1.

26. Sulway, M. J.; Malins, J. M. ACETONE IN DIABETIC KETOACIDOSIS. *Lancet* **1970**, *296*, 736–740, doi:10.1016/S0140-6736(70)90218-7.

27. Minh, T. D. C.; Oliver, S. R.; Ngo, J.; Flores, R.; Midyett, J.; Meinardi, S.; Carlson, M. K.; Rowland, F. S.; Blake, D. R.; Galassetti, P. R. Noninvasive measurement of plasma glucose from exhaled breath in healthy and type 1 diabetic subjects. *Am. J. Physiol. Endocrinol. Metab.* **2011**, *300*, E1166-75, doi:10.1152/ajpendo.00634.2010.

28. Galassetti, P. R.; Novak, B.; Nemet, D.; Rose-Gottron, C.; Cooper, D. M.; Meinardi, S.; Newcomb, R.; Zaldivar, F.; Blake, D. R. Breath Ethanol and Acetone as Indicators of Serum Glucose Levels: An Initial Report. *Diabetes Technol. Ther.* **2005**, *7*, 115–123, doi:10.1089/dia.2005.7.115.

29. Lee, J.; Ngo, J.; Blake, D.; Meinardi, S.; Pontello, A. M.; Newcomb, R.; Galassetti, P. R. Improved predictive models for plasma glucose estimation from multi-linear regression analysis of exhaled volatile organic compounds. *J. Appl. Physiol.* **2009**, *107*, 155–160, doi:10.1152/japplphysiol.91657.2008.

30. Qin, T.; Xu, X.; Polák, T.; Pacáková, V.; Štulík, K.; Jech, L. A simple method for the trace determination of methanol, ethanol, acetone and pentane in human breath and in the ambient air by preconcentration on solid sorbents followed by gas chromatography. *Talanta* **1997**, *44*, 1683–1690, doi:10.1016/S0039-9140(97)00073-8.

31. Turner, C.; Španěl, P.; Smith, D. A longitudinal study of ammonia, acetone and propanol in the exhaled breath of 30 subjects using selected ion flow tube mass spectrometry, SIFT-MS. *Physiol. Meas.* **2006**, *27*, 321–337, doi:10.1088/0967-3334/27/4/001.

32. Schmidt, F. M.; Vaittinen, O.; Metsälä, M.; Lehto, M.; Forsblom, C.; Groop, P.-H.; Halonen, L. Ammonia in breath and emitted from skin. *J. Breath Res.* **2013**, *7*, 017109, doi:10.1088/1752-7155/7/1/017109.

33. Matatagui, D.; Sainz-Vidal, A.; Gràcia, I.; Figueras, E.; Cané, C.; Saniger, J. M. Chemoresistive gas sensor based on ZIF-8/ZIF-67 nanocrystals. *Sensors Actuators B Chem.* **2018**, *274*, 601–608, doi:10.1016/J.SNB.2018.07.137.

34. Pan, Y.; Liu, Y.; Zeng, G.; Zhao, L.; Lai, Z. Rapid synthesis of zeolitic imidazolate framework-8 (ZIF-8) nanocrystals in an aqueous system. *Chem. Commun.* **2011**, *47*, 2071, doi:10.1039/c0cc05002d.

35. Gross, A. F.; Sherman, E.; Vajo, J. J. Aqueous room temperature synthesis of cobalt and zinc sodalite zeolitic imidizolate frameworks. *Dalt. Trans.* **2012**, *41*, 5458, doi:10.1039/c2dt30174a.

36. Sahu, S. R.; Devi, M. M.; Mukherjee, P.; Sen, P.; Biswas, K. Optical Property Characterization of Novel Graphene-X (X=Ag, Au and Cu) Nanoparticle Hybrids. *J. Nanomater.* **2013**, *2013*, 1–9, doi:10.1155/2013/232409.

37. Park, K. S.; Ni, Z.; Côté, A. P.; Choi, J. Y.; Huang, R.; Uribe-Romo, F. J.; Chae, H. K.; O'Keeffe, M.; Yaghi, O. M. Exceptional chemical and thermal stability of zeolitic imidazolate frameworks. *Proc. Natl. Acad. Sci. U. S. A.* **2006**, *103*, 10186–10191, doi:10.1073/pnas.0602439103.

38. Matatagui, D.; Sainz-Vidal, A.; Gràcia, I.; Figueras, E.; Cané, C.; Saniger, J. M. Chemoresistive gas sensor based on ZIF-8/ZIF-67 nanocrystals. *Sensors Actuators, B Chem.* **2018**, *274*, doi:10.1016/j.snb.2018.07.137.